Development 134, 455-465 (2007) doi:10.1242/dev.02744

Regulation of redox metabolism in the mouse oocyte and embryo

Rémi Dumollard[1,2,*], Zoe Ward[2], John Carroll[2] and Michael R. Duchen[2]

Energy homeostasis of the oocyte is a crucial determinant of fertility. Following ovulation, the oocyte is exposed to the unique environment of the Fallopian tube, and this is reflected in a highly specialised biochemistry. The minute amounts of tissue available have made the physiological analysis of oocyte intermediary metabolism almost impossible. We have therefore used confocal imaging of mitochondrial and cytosolic redox state under a range of conditions to explore the oxidative metabolism of intermediary substrates. It has been known for some time that the early mouse embryo metabolises external pyruvate and lactate but not glucose to produce ATP. We now show at the level of single oocytes, that supplied glucose has no effect on the redox potential of the oocyte. Pyruvate is a cytosolic oxidant but a mitochondrial reductant, while lactate is a strong cytosolic reductant via the activity of lactate dehydrogenase. Unexpectedly, lactate-derived pyruvate appears to be diverted from mitochondrial oxidation. Our approach also reveals that the level of reduced glutathione (GSH) in the oocyte is maintained by glutathione reductase, which oxidises intracellular NADPH to reduce oxidised glutathione. Surprisingly, NADPH does not seem to be supplied by the pentose phosphate pathway in the unfertilised oocyte but rather by cytosolic NADP-dependent isocitrate dehydrogenase. Remarkably, we also found that the oxidant action of pyruvate impairs development, demonstrating the fundamental importance of redox state on early development.

KEY WORDS: Mouse, Oocyte, Autofluorescence, NAD(P)H, Oxido-reduction, Mitochondria

INTRODUCTION

Following ovulation, mammalian oocytes and embryos rely on internal stores and on the few metabolites supplied by secretions of the Fallopian tube to survive. The ability of the preimplantation embryo to maintain an appropriate metabolism is necessary for successful implantation. Since the 1960s, it has been possible to culture mammalian embryos in vitro before being re-implanted and give rise to normal offspring (Gardner et al., 2002), but the development of a chemically defined culture medium supporting development from fertilisation until blastocyst stage took decades of research (Summers and Biggers, 2003). Today, even though empirically defined in vitro culture conditions allow development until the blastocyst stage, the regulation of intermediary metabolism in the mammalian early embryo is still poorly understood.

Numerous biochemical studies investigating the substrate requirements of mammalian embryos suggest that they possess a very specific intermediary metabolism, which is strictly regulated during early development (Biggers et al., 1967; Summers and Biggers, 2003; Johnson et al., 2003; Gardner et al., 2002; Leese, 2002). It is long known that pyruvate supports development from fertilisation, whereas lactate supports development from the two-cell stage on and glucose can support early development only after compaction (Leese, 1995; Leese, 2002). While such a pattern of substrate utilisation supports sufficient ATP production and biosynthetic pathways in the early embryo, neither the reasons nor the mechanisms for this highly regulated pattern of substrate utilisation have been elucidated. Intermediary metabolism also produces the electron donors NADH and NADPH, which, besides being used for energetic and biosynthetic metabolism, sets the intracellular redox potential (or redox state) of the embryo and may thereby have an impact on early development.

The pyridine nucleotides NADH and NADPH and the thiol tripeptide glutathione (γ-glutamylcysteinylglycine, GSH) form the vast majority of the reducing equivalents available in the cell. GSH is the major antioxidant system in the cell (Dickinson and Forman, 2002), while NADH and NADPH (NAD(P)H) are direct antioxidant molecules (Kirsch and De Groot, 2001). However, whether NAD(P)H has an oxidant or antioxidant action in the cell depends on the specific enzymatic content of that cell. The metabolism of lactate, pyruvate and glucose can potentially provide NAD(P)H and ATP in the cytosol as well as inside the mitochondria (Fig. 1). However, even though the impact of these substrates on ATP production is now known (Biggers et al., 1967; Houghton et al., 1996; Leese, 2002; Johnson et al., 2003), their impact on the cytosolic and the mitochondrial redox potential remain largely unexplored. Moreover, biochemical characterisation of the enzymatic activities present in the early embryo suggests that each of these substrates may be metabolised by multiple pathways (Cetica et al., 2002; Comizzoli et al., 2003; Johnson et al., 2003; Biggers et al., 1967; Barbehenn et al., 1974; Leese, 2002) (Fig. 1). However, due to the paucity of studies of the intracellular redox metabolism in live oocytes and embryos (Lane and Gardner, 2000), the metabolic pathways operating during mammalian early development to regulate intracellular NAD(P)H levels are mostly unknown.

Oxidative stress, mediated by reactive oxygen species (ROS), results in an imbalance of the intracellular redox potential towards an oxidised potential (Balaban et al., 2005). Oxidative stress has been found to be associated with impaired early development and fragmented embryos (Johnson and Nasr-Esfahani, 1994; Yang et al., 1998); it can induce apoptosis of the oocyte and early embryo (Liu and Keefe, 2000; Liu et al., 2000) and is associated with maternal

[1]Laboratoire de Biologie du Développement UMR 7009 CNRS/Paris VI, Observatoire, Station Zoologique, Villefranche sur Mer, 06230 France. [2]Department of Physiology, University College London, Gower Street, London WC1E 6BT, UK.

*Author for correspondence (e-mail: remi.dumollard@obs-vlfr.fr)

Accepted 14 November 2006

aging and postovulatory aging of the egg (Fissore et al., 2002; Tarin, 1996). Understanding how mammalian intermediary metabolism regulates the intracellular redox potential (and hence antioxidant defence) is thus of fundamental importance.

Finally, the role of redox potential during early development has been studied only under the perspective of oxidative stress, but the role of the redox potential per se is still unknown. Recent studies have revealed that NAD(P)H and its oxidised counterpart $NAD(P)^+$ as well as GSH are direct modulators of numerous enzymes (Dickinson and Forman, 2002; Imai et al., 2000; Zhang et al., 2002; Ghezzi, 2005; Nutt et al., 2005; Liu et al., 2005). As some of these enzymes are expressed in oocytes and early embryos (McBurney et al., 2003; Hildebrand and Soriano, 2002; Nutt et al., 2005), mammalian early development might well be regulated by the intracellular redox potential itself (for a review, see Dumollard et al., 2006b). Herein lies another reason to characterise the redox metabolism operating in the oocyte and embryo and its impact on development.

We have monitored intracellular NAD(P)H and GSH levels together with the mitochondrial redox state in single mouse oocytes and embryos to study the regulation of redox potential by exogenous substrates. We have also used a pharmacological approach to characterise which metabolic pathways regulate the intracellular redox potential. Finally the effect of manipulations of the redox potential on preimplantation development has been assessed.

MATERIALS AND METHODS

Oocytes and embryos

Mature (MII) oocytes were recovered from 21-24-day-old MF1 outbred mice previously administered 7 i.u. of pregnant mare serum gonadotrophin (PMSG, Intervet, UK) and 5 i.u. human chorionic gonadotrophin (hCG, Intervet, UK) at a 48-hour interval. Mice were culled by cervical dislocation and the oviducts removed 14-16 hours post-hCG. Cumulus masses were released into HEPES-buffered KSOM supplemented with amino acids [H-KSOM/AA, made in the laboratory (Biggers et al., 2000)] containing 1 mg/ml BSA by rupture of the oviduct with a 27 gauge needle. When it was necessary to remove the cumulus cells, hyaluronidase (150 i.u. ml^{-1}, Sigma) was added to the H-KSOM/AA. Cumulus-free oocytes were collected and washed in H-KSOM/AA three times and placed in a drop of the same medium under mineral oil (Dow Corning, UK).

Germinal vesicle (GV) oocytes were recovered by direct dissection of ovaries removed from mice primed with 7 i.u. PMSG 48 hours before. GV oocytes were then cultured in H-KSOM/AA until imaging (typically 30 minutes to 5 hours of culture).

In our laboratory, mouse embryos are routinely cultured in KSOM/AA medium containing 0.2 mmol/l glucose, 0.2 mmol/l pyruvate and 10 mmol/l lactate. Such KSOM/AA medium supports development from fertilisation to blastocyst (Biggers et al., 2000) (Fig. 8). For embryo culture, one-cell (pronuclei stage) embryos were collected from hormone-primed mice 27-28 hours post-hCG. They were washed twice in 120 μl drops of fresh H-KSOM/AA. They were then washed three times in 120 μl of the prospective KSOM/AA media (Biggers et al., 2000) in which they were to be cultured, and finally transferred in groups of 15-30 to pre-equilibrated (5% CO_2 in 95% air, 37°C) 60 μl drops of the relevant KSOM/AA media under mineral oil (Dow Corning, UK) and placed in a water jacketed 37°C incubator (Kendro, UK). All embryos were cultured for 5 days until the stage of development was scored.

Subcellular analysis of autofluorescence imaging

The autofluorescence of mouse oocytes and embryos was imaged by confocal or epifluorescence microscopy essentially as previously described (Duchen et al., 2003; Dumollard et al., 2003; Dumollard et al., 2004; Dumollard et al., 2006b). Blue autofluorescence – emitted by the pyridine nucleotides NADH and NADPH in their reduced form – was excited with UV light (360 or 351 nm on the CLSM) and emission was collected using a 470 nm longpass or a 435-485 nm bandpass filter (for CLSM). NAD(P)H autofluorescence is located both in mitochondria and in the cytosol (Dumollard et al., 2004; Dumollard et al., 2006b) (Fig. 1).

The fluorescence of oxidised flavoproteins (FAD^{++}) was excited using the 458 nm line of an argon laser or with a 440-490 nm bandpass filter, whereas emitted fluorescence was collected through either a 520 nm longpass filter or a 505-550 nm bandpass filter. The autofluorescence derived from oxidised flavoproteins (FAD^{++}) is exclusively localised into the mitochondria (Dumollard et al., 2004; Dumollard et al., 2006b) (Fig. 1). The organisation of the GV oocyte, which presents a large nucleus (the GV) surrounded by mitochondria (Dumollard et al., 2006a; Dumollard et al., 2006b) (see FAD^{++} image in Fig. 2B and Fig. 3A), allows recording of a pure nuclear signal (i.e. devoid of mitochondria, dotted line in Fig. 3A) used to estimate the cytosolic redox potential and recording of a mitochondrial redox potential by monitoring changes of fluorescence in a small perinuclear region of interest (ROI) enriched in mitochondria (dark blue line plotted in Fig. 3A).

Quantitative analysis of the images obtained was done using the Metamorph (Universal Imaging, USA) and the Zeiss LSM 510 software.

Measurement of intracellular GSH

After the autofluorescence imaging, the increase in MCB fluorescence (exc: 360 nm; em: 470 nm longpass) of oocytes incubated in 12.5 μmol/l MCB was continuously imaged for 40 to 90 minutes until a plateau was observed (for details, see Keelan et al., 2001). In order to compare experiments done on different days, the level of GSH fluorescence is expressed as a percentage of the fluorescence emitted from a control embryo (untreated M2 oocyte or GV oocyte) imaged simultaneously. For treatment with inhibitors, oocytes and embryos were cultured in the relevant drug for 10 minutes to 5 hours before being imaged in a drop of control H-KSOM/AA.

Chemicals

D(+)Glucose, 2-deoxyglucose, DL-Lactic acid, pyruvate, oxamate, oxalomalate, dehydroisoandrosterone (DHEA), FCCP, CN-, rotenone, CIN, dimethyl malate, BCNU [1,3-bis(2-chloroethyl)-1-nitrosourea] and TEMPO (2,2,6,6-tetramethylpiperidine-1-oxy) are all from Sigma, UK. During autofluorescence imaging experiments these chemicals were added as 10× solution of their final concentration (indicated under the graphs).

RESULTS

Impact of glucose, pyruvate and lactate on the intracellular redox potential in the mouse oocyte

To establish how metabolism of energetic substrates sustains the intracellular redox potential, we imaged mature mouse oocytes and fully grown GV oocytes immediately following transfer to KSOM/AA medium devoid of glucose (G), lactate (L) and pyruvate (P) (2 minutes before imaging was started) before adding each substrate one by one. Fig. 2A shows that removal of G, L and P from the medium provoked a decline in NAD(P)H autofluorescence, whereas FAD^{++} autofluorescence was not affected. Even in the presence of glucose, NAD(P)H levels decreased (Fig. 2C, Fig. 3A). After NAD(P)H reached a new steady state level (15 to 20 minutes after onset of substrate deprivation), glucose at 25 times its normal concentration was added to the observation chamber but had absolutely no effect on either autofluorescence signal (Fig. 2A). To confirm that glucose is not metabolised in mouse oocytes, we incubated maturing GV oocytes for 3 hours in complete H-KSOM/AA containing 4 mmol/l glucose and 8 mmol/l 2-deoxyglucose (a competitive inhibitor of glucose metabolism) and found that global NAD(P)H autofluorescence was not significantly different than in control oocytes (107.2±6.0% of control, $P<0.591$, $n=35$ oocytes).

These observations are consistent with the finding that glycolysis is blocked in mouse oocytes (Barbehenn et al., 1974). Published data suggest that glucose might be metabolised via the pentose phosphate pathway [PPP, which generates NADPH (Fig. 1) (Downs et al.,

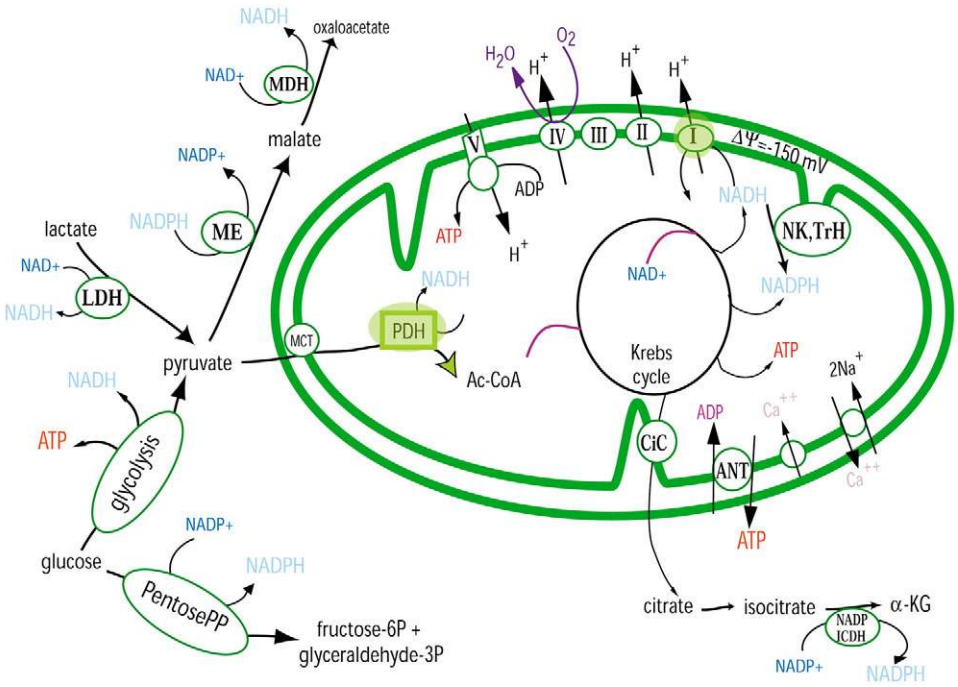

Fig. 1. NAD(P)H and FAD^{++} autofluorescence originate from both mitochondrial and cytosolic compartments in mouse oocytes. Schematic representation of the metabolic pathways producing NADH and NADPH in the cytosol and the mitochondria of a eukaryotic cell. The possible sources of FAD^{++} fluorescence in the mouse oocyte are highlighted in green and are the pyruvate dehydrogenase (PDH) complex and the complex I of the mitochondrial electron transport chain. See main text for details. α-KG, alpha-ketoglutarate; Ac-CoA, acetyl coenzyme A; ANT, adenine nucleotide translocase; CiC, citrate carrier; LDH, lactate dehydrogenase; ME, malic enzyme; MDH, malate dehydrogenase; MCT, mono carboxylate transporter; NAD(P)$^+$, oxidised nicotinamide adenine dinucleotide (phosphate); NADH, reduced nicotinamide adenine dinucleotide, NADP-ICDH, NADP-dependent isocitrate dehydrogenase; NK, NAD kinase; PentosePP, pentose phosphate pathway, TrH, transhydrogenase.

1998; Urner and Sakkas, 2005; Comizzoli et al., 2003)]. To test this possibility, we imaged mouse oocytes incubated in complete KSOM/AA medium and applied the PPP inhibitor DHEA (Nutt et al., 2005). DHEA provoked an increase in global NAD(P)H mirrored by a decrease in FAD^{++} autofluorescence, but cytosolic NAD(P)H (dashed blue line in Fig. 2B) remained unchanged (Fig. 2B). This observation suggests that DHEA unexpectedly inhibits mitochondrial respiration in mouse oocytes [as has been observed in some preparations (Correa et al., 2003)] and suggests that the PPP does not supply NADPH in unfertilised mouse oocytes. This result was confirmed by inhibiting PPP with another unrelated inhibitor (6-aminonicotinamide) that did not change NAD(P)H or FAD^{++} autofluorescence at all (n=9, data not shown). Therefore it seems that glucose metabolism does not impact the intracellular redox potential in mouse oocytes.

By contrast to glucose, pyruvate addition (0.4 mmol/l) decreased both NAD(P)H and FAD^{++} fluorescence signals, whereas lactate (10 mmol/l) provoked a sharp increase in NAD(P)H autofluorescence without affecting that of FAD^{++} (Fig. 2A,C). As pyruvate seemed to affect both cytosolic and mitochondrial redox state, we further investigated the effect of pyruvate by analysing specific changes in cytosolic and mitochondrial NAD(P)H pools (see Materials and methods; Fig. 3A). During substrate deprivation, global, nuclear and mitochondrial NAD(P)H signals decreased, suggesting that depletion of substrates decreased both mitochondrial and cytosolic NAD(P)H. Upon pyruvate addition, the global NAD(P)H signal decreased and the distribution of the NAD(P)H signal changed drastically from a diffuse distribution to a more punctate one reminiscent of mitochondrial distribution (compare t=0' or 24' with t=34' in Fig. 3A). The linear fluorescence profiles (under the images in Fig. 3A) show more clearly that, after pyruvate addition, the signal from some areas decreased while others increased in intensity. These areas of high NAD(P)H autofluorescence correspond to mitochondria as NAD(P)H was further increased in these areas by addition of the mitochondrial inhibitors rotenone and cyanide. Therefore, while pyruvate oxidises NAD(P)H in the cytosol it promotes reduction of mitochondrial NAD(P)$^+$.

The role of lactate dehydrogenase (LDH) in the response to lactate was explored using oxamate, a specific competitive inhibitor of LDH (Wilkinson and Walter, 1972). Fig. 2C shows that NAD(P)H increased after lactate addition and the subsequent addition of oxamate decreased NAD(P)H autofluorescence very sharply (Fig. 2C). Increasing further lactate in the medium in the presence of oxamate had no effect on the NAD(P)H signals. Thus, lactate directly reduces the cytosolic redox potential (i.e. increases cytosolic NADH) via the action of LDH.

To confirm the observed effects of pyruvate on the cytosolic redox potential we blocked LDH (with oxamate, Fig. 3B) or mitochondrial respiration (Fig. 4A) before adding pyruvate. Oxamate prevented the pyruvate-induced decrease in global NAD(P)H without preventing the reduction of FAD^{++}, whereas inhibiting mitochondrial respiration had no effect on the response to pyruvate (Fig. 4A). In addition, mitochondrial NAD(P)H increased upon pyruvate addition when LDH was blocked, further establishing that exogenous pyruvate stimulates mitochondrial NAD(P)H production (Fig. 3B compared with Fig. 3A). These observations demonstrate that

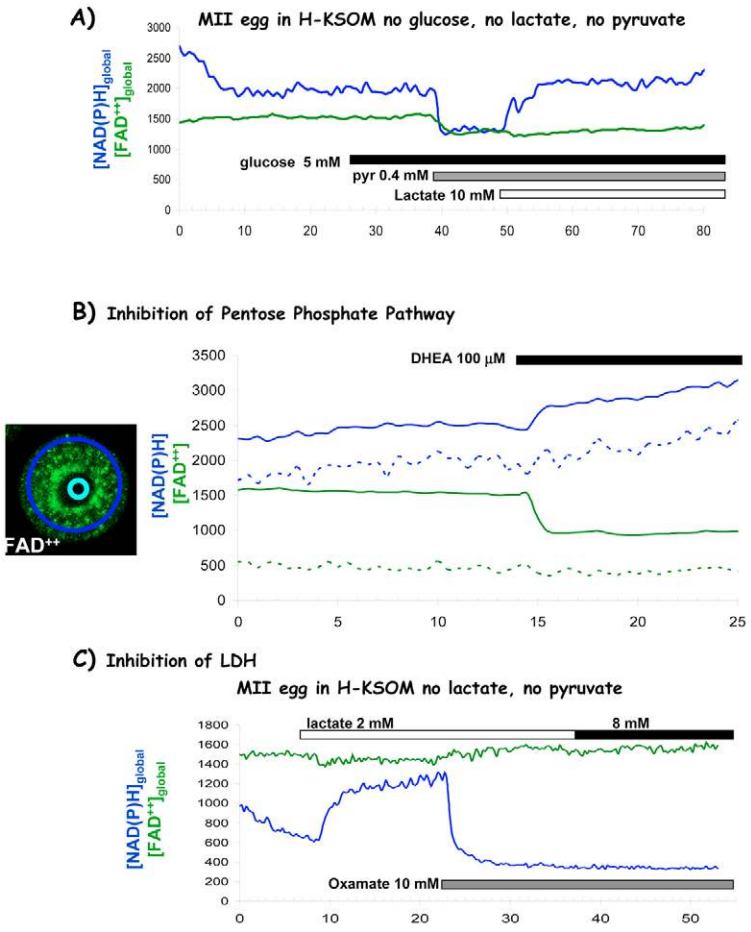

Fig. 2. Glucose, pyruvate and lactate have distinct effects on NAD(P)H and FAD^{++} autofluorescence, indicating distinct metabolic pathways. (**A**) Timecourse of changes in NAD(P)H (blue) and FAD^{++} (green) autofluorescence in a MII oocyte incubated at time 0 in H-KSOM/AA that was devoid of glucose, lactate and pyruvate (*n*=35 oocytes). These substrates were added at the times indicated at the bottom of the graph. (**B**) Inhibition of the pentose phosphate pathway: timecourse of changes in autofluorescence in a fully grown GV oocyte incubated in complete H-KSOM/AA (*n*=12 oocytes). The PPP inhibitor DHEA was added to the chamber at the time indicated at the top of the graph. Continuous traces indicate global signals (large, dark-blue ROI in the FAD^{++} image). Dashed traces indicate nuclear signals (small, light-blue ROI in the FAD^{++} image, left). (**C**) Inhibition of LDH: timecourse of changes in autofluorescence in a mature MII oocyte incubated in H-KSOM/AA without lactate or pyruvate (*n*=18 oocytes). Lactate (2 mmol/l) was added, as indicated, followed by the addition of the LDH inhibitor, oxamate (10 mmol/l). The concentration of lactate in the medium was then increased to 8 mmol/l, as indicated. The *x*-axes indicate time in minutes.

pyruvate and lactate are metabolised in the cytosol by LDH to set the cytosolic redox potential and that exogenous pyruvate (but, surprisingly, not lactate-derived pyruvate) is also metabolised in the mitochondria.

Impact of pyruvate metabolism on intracellular redox potential

Thus, pyruvate is metabolised both in the cytosol and in the mitochondria of mouse oocytes. We therefore explored the influence of the mitochondrial metabolism of pyruvate on the redox potential (Fig. 4B,C). Transport of pyruvate from the cytosol into mitochondria is blocked by a low concentration of α-cyano-4-hydroxy cinnamate (CIN) (Del Prete et al., 2004). Application of CIN (0.5 mmol/l) to mature mouse oocytes incubated in complete KSOM/AA decreased global NAD(P)H autofluorescence and increased FAD^{++} autofluorescence (Fig. 4B). Subsequent addition of pyruvate failed to generate the expected change in FAD^{++}, whereas NAD(P)H autofluorescence still decreased, consistent with pyruvate entry into the cytosol but not into mitochondria (Fig. 4B).

The decrease in NAD(P)H autofluorescence induced by CIN could be either due to accumulation of pyruvate in the cytosol, which then oxidises NADH via LDH, or to inhibition of the mitochondrial Krebs cycle (see Fig. 1). To discriminate between these, LDH was inhibited by oxamate before addition of CIN (Fig. 4C). This prevented the decrease in NAD(P)H caused by CIN while FAD^{++} was still oxidised. Subsequent addition of pyruvate no longer changed either NAD(P)H or FAD^{++} signals. These data together suggest that, in the mature mouse oocyte, exogenous pyruvate may be imported directly into mitochondria to fuel the Krebs cycle, but may also be metabolised by LDH in the cytosol.

Alternate sources of NAD(P)H operating in the mouse oocyte

The observations described so far suggest that the main roles of metabolic substrates present in culture media are to set the cytosolic NADH:NAD$^+$ ratio (via LDH). However, as alternate sources of NAD(P)H could contribute to the regulation of intracellular redox potential, we investigated further the sources of NAD(P)H in mouse oocytes (Fig. 5). Malate can be metabolised by malic enzyme (ME, cytosolic) and by malate dehydrogenase (MDH, cytosolic and mitochondrial) to produce NADPH and NADH respectively (Fig. 1) (Stryer, 1970). Addition of the permeant malate analogue dimethyl malate (Me_2-malate) provoked a consistent decrease in FAD^{++} autofluorescence without significantly affecting global NAD(P)H autofluorescence (Fig. 5A). This observation suggests that Me_2-malate is mostly metabolised in mitochondria and that cytosolic MDH and ME are poorly active in mouse oocytes (Fig. 5A). It also contradicts somehow the recent finding that cytosolic MDH is expressed in mouse oocytes (Lane and Gardner, 2005).

As neither the PPP (Fig. 2) nor ME (Fig. 5A) supply NADPH in mouse oocytes, we hypothesised that cytosolic NADP-ICDH – an important provider of cytosolic NADPH in some somatic cells (Mallet and Sun, 2003; McDonald et al., 2005) – could serve this task. Inhibition of NADP-ICDH by oxalomalate (Yang and Park, 2003), applied to mouse oocytes incubated in complete KSOM/AA

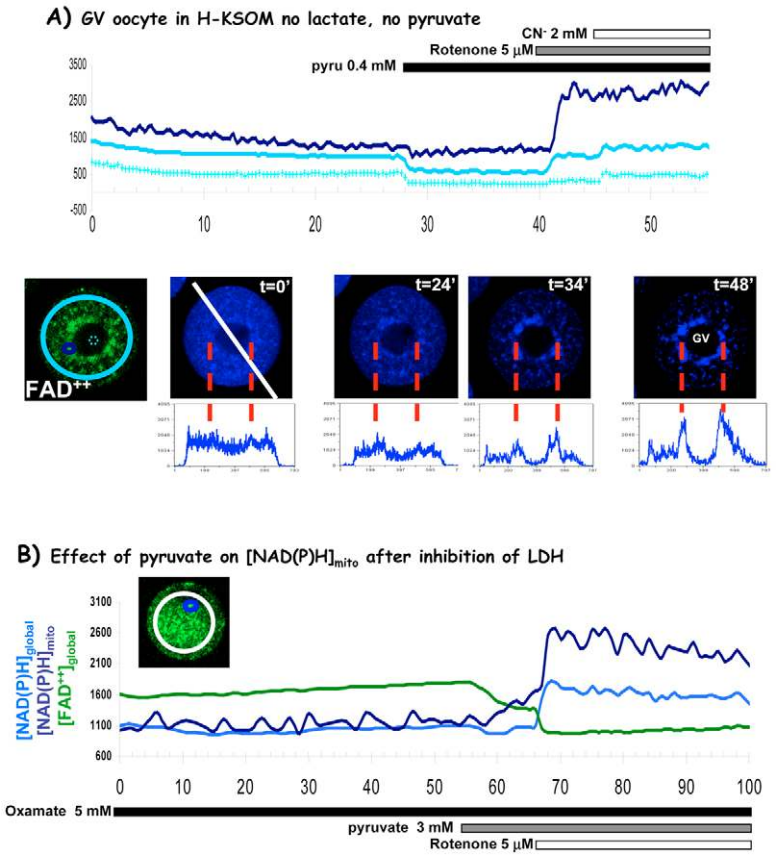

Fig. 3. Pyruvate causes the oxidation of cytosolic NADPH, but also a reduction in mitochondrial NAD(P)$^{+}$ and FAD^{++}. (**A**) Changes in NADH autofluorescence signal derived from measured global [large; light-blue ROI indicated on FAD^{++} image (below, left); thick light-blue trace], nuclear (small; dotted ROI in FAD^{++} image; bottom light-blue trace) and mitochondrial areas (small; dark-blue ROI in FAD^{++} image; dark-blue trace) in a fully grown GV oocyte. The cell was incubated at time 0 in H-KSOM/AA alone; pyruvate and mitochondrial reagents were added as indicated at the top of the graph (n=19 oocytes). The FAD^{++} image shows the oocyte analysed and the regions of interest used to plot the graph, as this clearly shows the distribution of mitochondria. (Below graph) NAD(P)H images of the oocyte collected at different times. White line in the image at t=0≦ indicates the line of the scan in the graphs shown below each image. The line-scan analysis reveals subcellular differences in the distribution of the changing NAD(P)H signal to the manipulations. Time indicated in minutes. (**B**) Effect of pyruvate on global FAD^{++} (large white ROI, green trace) and NAD(P)H (large white ROI, light blue trace) and on mitochondrial NAD(P)H (small blue ROI, dark blue trace) autofluorescence in an MII oocyte incubated in complete H-KSOM/AA containing 5 mmol/l oxamate (n=11 oocytes). Pyruvate and rotenone are added as indicated. The x-axes indicate time in minutes.

(Fig. 5B,C) also provoked a decrease in global and cytosolic NAD(P)H autofluorescence without affecting FAD^{++} autofluorescence (FCCP was added at the end of the experiment to completely oxidise the mitochondrial pools). This suggests that cytosolic NADPH levels are maintained by oxidation of isocitrate by cytosolic NADP-ICDH (Fig. 1).

Surprisingly, addition of oxamate after the oxalomalate-induced decrease in NAD(P)H failed to decrease further NAD(P)H, as opposed to the consistent decrease in NAD(P)H autofluorescence observed when oxamate is applied alone (n=35, Fig. 2C, Fig. 4C). As oxamate should affect the supply of cytosolic NADH exclusively (Wilkinson and Walter, 1972) and oxalomalate should affect the supply of cytosolic NADPH only (Yang and Park, 2003), the sequential addition of these two inhibitors are expected to have additive effects on NAD(P)H autofluorescence. Oxamate was added before oxalomalate to further test this hypothesis (Fig. 5C). Here again, inhibiting NADP-ICDH had no effect on NAD(P)H autofluorescence once LDH had been inhibited. Together, these observations indicate that, somehow, cytosolic NADH and NADPH pools are in equilibrium in the mouse oocyte.

Changes in NAD(P)H and in GSH during maturation and after fertilisation

An important role for NADPH in cells is to fuel the reduction of the thiol-containing glutathione by glutathione reductase (GR) (Fig. 7) and the glutaredoxin (Grx) system (Holmgren et al., 2005). We thus imaged intracellular NAD(P)H, FAD^{++} and GSH in the same oocyte to study how NAD(P)H regulates the levels of GSH in the mouse embryo (Fig. 6). Intracellular reduced glutathione (GSH) can be measured by imaging the fluorescent adduct formed with monochlorobimane (MCB) [see Keelan et al. (Keelan et al., 2001) for details on MCB]. First, to validate our GSH imaging technique and to assess how oxidising GSH impacts autofluorescence levels, we inhibited GSH reduction by GR (with BCNU) (Gardiner and Reed, 1995a) or oxidised GSH directly [by a short incubation in diamide (Kosower and Kosower, 1995; Akella and Harris, 1999)] and measured autofluorescence and GSH levels (Fig. 6A). Fig. 6A shows, as expected, that inhibiting GR significantly decreased GSH levels (to 23.1±2.9% of untreated oocytes, P<0.0003, n=28 oocytes), whereas oxidising GSH with diamide decreased GSH levels to 30.9±4.4% of untreated controls (n=10 oocytes, P<0.0004, Fig. 6A). However, BCNU and diamide have strikingly dissimilar effects on the autofluorescence signal: BCNU slightly but significantly increased NAD(P)H (107.1±0.8% of untreated controls, P<0.019, n=28 oocytes) without affecting mitochondrial FAD^{++} (Fig. 6A). By contrast, diamide significantly oxidised both NAD(P)H (observed as a decrease of fluorescence, 74.8±5.8%, P<0.012, n=10 oocytes) and FAD^{++} (observed as an increase of fluorescence, 118.0±2.2%, P<0.004, n=10 oocytes). The acute application of diamide (15 minutes incubation) used in our protocol mostly oxidises GSH, and to a lesser extent protein thiols, but not NAD(P)H directly (Kosower and Kosower, 1995). Our observations therefore suggest that, in mature mouse oocytes, NADPH is used by GR to maintain GSH levels.

Then we determined the relationship between NAD(P)H, FAD^{++} and GSH during development by measuring them in oocytes before maturation (GV oocytes) and after maturation (M2 oocytes) as well as in two-cell embryos (Fig. 6B). Fig. 6B shows that FAD^{++} autofluorescence did not vary during the developmental stages considered, whereas NAD(P)H was constant during maturation but decreased significantly between fertilisation and the two-cell stage (to 65.9±0.9% of mature oocytes, P<0.012, n=12 oocytes). By

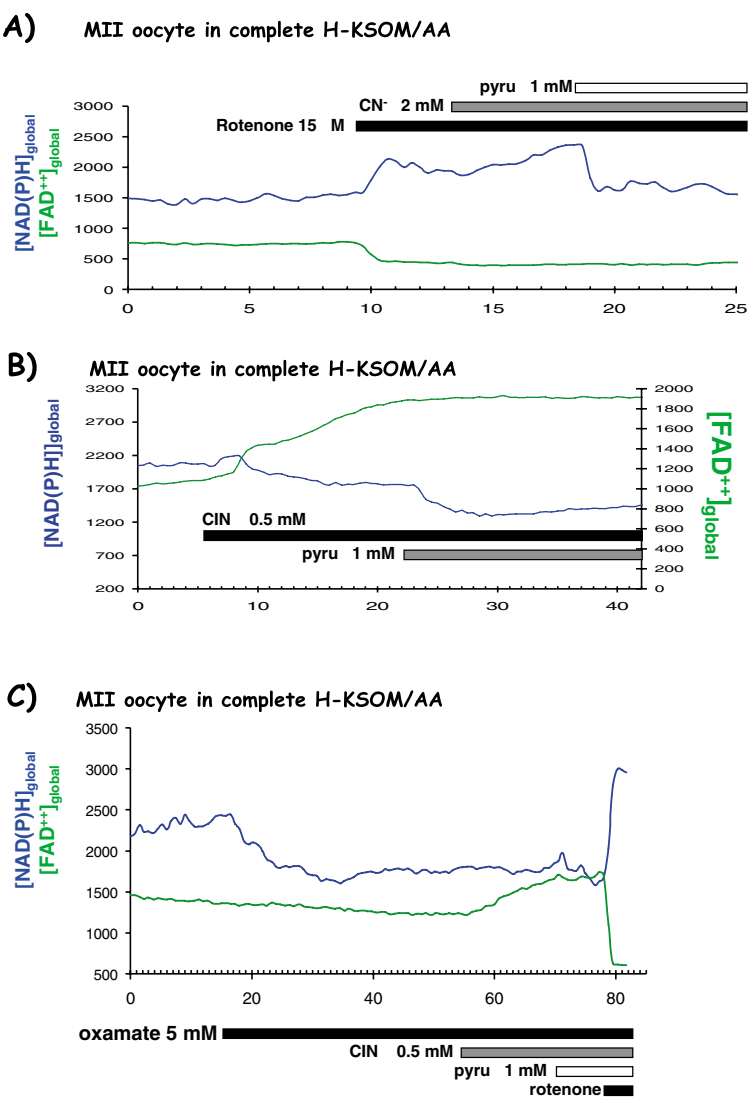

Fig. 4. Effect on global autofluorescence of inhibition of mitochondrial respiration and pyruvate uptake. (**A**) Timecourse of changes in global NAD(P)H and FAD^{++} autofluorescence in a mature MII oocyte incubated in H-KSOM/AA alone (*n*=18 oocytes). Pyruvate is added after inhibition of mitochondrial respiration with rotenone and cyanide (CN^-, as indicated). (**B**) Timecourse of changes in global NAD(P)H and FAD^{++} autofluorescence in a mature MII oocyte after cinnamate (CIN) perfusion (*n*=15 oocytes). The efficacy of CIN as an inhibitor of mitochondrial pyruvate uptake is confirmed by the lack of effect of the subsequent addition of pyruvate on FAD^{++} autofluorescence. (**C**) Effect of CIN perfusion on global autofluorescence of a mature MII oocyte after inhibition of LDH with oxamate (*n*=12 oocytes). Rotenone was added to a final concentration of 15 μmol/l. The *x*-axes indicate time in minutes.

contrast, GSH increased during maturation (GSH levels before maturation being 64.4±2.4% of M2 oocytes, $P<0.002$, $n=25$ oocytes) and decreased after fertilisation (to 65.5±2.3% of M2 oocyte, $P<0.013$, $n=12$ oocytes), as found earlier in mammals (for a review, see Luberda, 2005). The concomitant decrease in NAD(P)H and GSH occurring after fertilisation suggests that GSH production is dependent on NADPH levels during this stage of development. On the contrary, the increase in GSH levels observed during maturation was not accompanied by an increase in NAD(P)H autofluorescence, suggesting that this increase in GSH during maturation does not rely on increased NADPH. These findings are reminiscent of the different GSH metabolisms of mouse oocytes before and after fertilisation (see Gardiner and Reed, 1995a; Gardiner and Reed, 1995b).

Impact of redox potential in early development

We next examined how manipulations of the redox potential affect preimplantation development. We cultured one-cell embryos produced in vivo for 5 days in different KSOM/AA media resulting in different intracellular redox potential and determined the rate of blastocyst production in each condition (Fig. 8). To change intracellular redox potential, we chose three differently modified KSOM/AA media: (1) KSOM/AA containing five times more pyruvate than control KSOM/AA (from 0.2 mmol/l to 1 mmol/l, Fig. 8A); (2) KSOM/AA containing 10 mmol/l oxamate (to decrease cytosolic NADH or NAD^+, Fig. 8B); (3) KSOM/AA containing 9 mmol/l oxalomalate (to decrease cytosolic NADPH or $NADP^+$, Fig. 8C).

Surprisingly, we found that increasing pyruvate in the medium was detrimental for development, as a significantly lower percentage of blastocysts was consistently obtained (23.8±3.5%, $n=87$ embryos, four replicates) compared with control conditions (66.5±1.4%, $n=95$ embryos, four replicates, $P<0.015$). Furthermore, the inhibition of development by 1 mmol/l pyruvate could be rescued by adding the membrane-permeant antioxidant TEMPO [48.9±2.6% of blastocysts, $n=94$ embryos, four replicates versus 23.8±3.5% with high pyruvate only, $P<0.005$ (Keelan et al., 2001)]. This observation demonstrates that such a concentration of pyruvate is not toxic by itself, as has been reported earlier (Wales and Whittingham, 1971), and indicates that an oxidant action of pyruvate inhibits development.

Decreasing the cytosolic NADH:NAD^+ ratio with oxamate or the cytosolic NADPH:$NADP^+$ ratio with oxalomalate both inhibited development significantly [oxamate: 23.3±4.9% ($n=83$, four

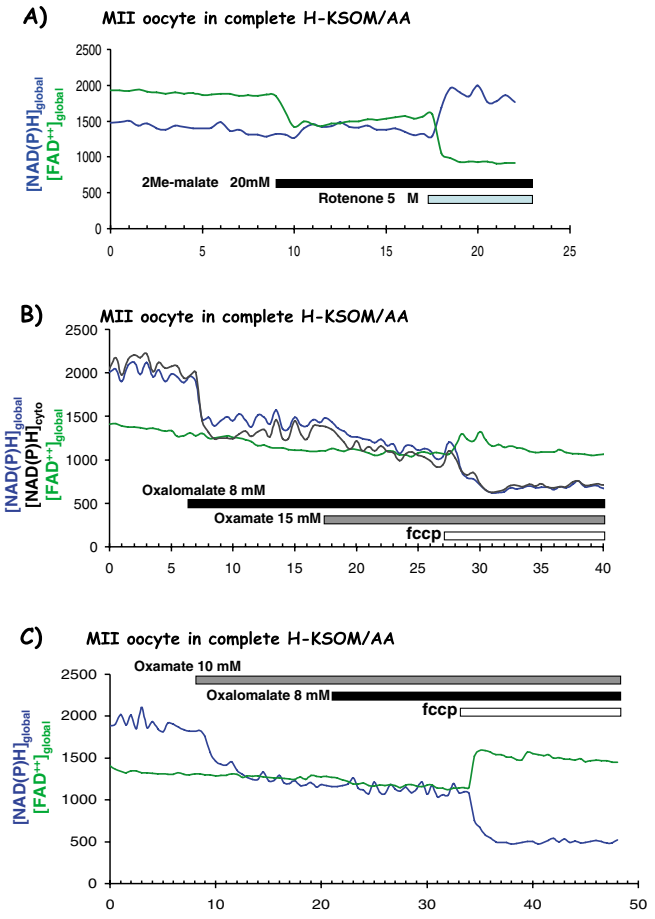

Fig. 5. NADP-ICDH but not malate metabolism regulates NAD(P)H levels in the mouse oocyte. (**A**) Timecourse of changes in global NAD(P)H and FAD^{++} autofluorescence in a mature MII oocyte incubated in H-KSOM/AA after perfusion of dimethyl-malate (2-Me-malate, *n*=7 oocytes). Rotenone was then added to inhibit mitochondria. (**B**) Timecourse of changes in global (light-blue trace) and cytosolic (black trace) NAD(P)H and of global FAD^{++} autofluorescence (green trace) in a mature MII oocyte incubated in H-KSOM/A after sequential addition of oxalomalate and oxamate (*n*=25 oocytes). (**C**) Timecourse of changes in global NAD(P)H (blue trace) and in global FAD^{++} autofluorescence (green trace) after sequential addition of oxamate and oxalomalate on a mature MII oocyte incubated in H-KSOM/A (*n*=25 oocytes). The *x*-axes indicate time in minutes.

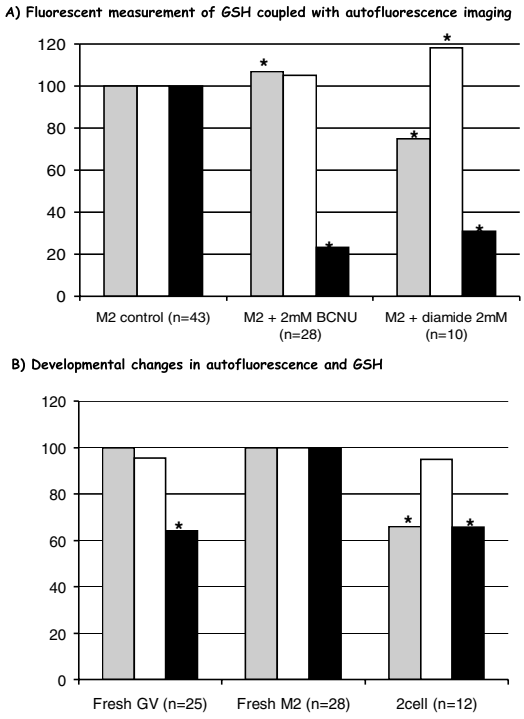

Fig. 6. Correlation between the level of GSH and the redox potential during development. (**A**) Relative amounts of NAD(P)H (grey bars), FAD^{++} (white bars) and GSH (black bars) in mature MII oocytes (M2 control), MII oocytes treated with 2 mmol/l BCNU for 1 hour (M2+ 2 mmol/l BCNU) and in MII oocytes treated with 2 mmol/l diamide for 15 minutes (M2+2 mmol/l diamide). The asterisks indicate that the values are significantly different from the control condition. (**B**) Relative amounts of NAD(P)H (grey bars), FAD^{++} (white bars) and GSH (black bars) in GV oocytes (fresh GV), in mature MII oocytes (fresh M2) and in two-cell embryos (2 cell). The asterisks indicate that the values are significantly different from the MII oocytes. *P*=0.019.

replicates) versus 65.5±5.1% (*n*=92 embryos, four replicates), *P*<0.009; oxalomalate: 5±2.5% (*n*=83 embryos, four replicates) versus 65.5±5.1% (*n*=69 embryos, four replicates), *P*<0.002]. These observations indicate that, in the mouse embryo, both cytosolic NADH and NAD^+ and NADPH and $NADP^+$ must be maintained to ensure proper early development.

DISCUSSION

This work was aimed at studying the redox metabolism of mouse oocytes and embryos at the single cell and subcellular levels. We used a non-invasive imaging strategy (Dumollard et al., 2003; Dumollard et al., 2004; Dumollard et al., 2006b) coupled with a pharmacological approach to decipher the mechanisms maintaining intracellular redox potential. Finally, we intervened to manipulate redox potential in order to examine its impact on early embryonic development.

Our observations reveal that an efficient enzymatic system regulates the levels of NADH and NAD^+, NADPH and $NADP^+$ and GSH and GSSG in mouse oocytes. This study also shows that the cytosolic and mitochondrial metabolism of exogenous substrates defines a redox potential that supports development to the blastocyst stage.

Intracellular metabolism of glucose in mouse oocytes

Our observations suggest that glucose is poorly metabolised in the mouse oocyte as neither the acute addition of glucose nor the specific inhibition of the pentose phosphate pathway (with 6-AN and DHEA) or of glucose metabolism (with 2-deoxyglucose) affect cytosolic NAD(P)H levels. This is in accord with previous observations that glycolysis is inhibited in mouse early embryos (Barbehenn et al., 1974; Leese, 2002; Johnson et al., 2003). However, several studies suggested that the pentose phosphate pathway (PPP) may be active in maturing oocytes and zygotes and may regulate oocyte maturation and early development (Cetica et al., 2002; Downs et al., 1998; Urner and Sakkas, 2005; Comizzoli et al., 2003). Our observations show that the PPP plays a minor role, if any, in the supply of NADPH in the unfertilised oocyte. Such a finding emphasises that the early mouse embryo has a metabolism that is

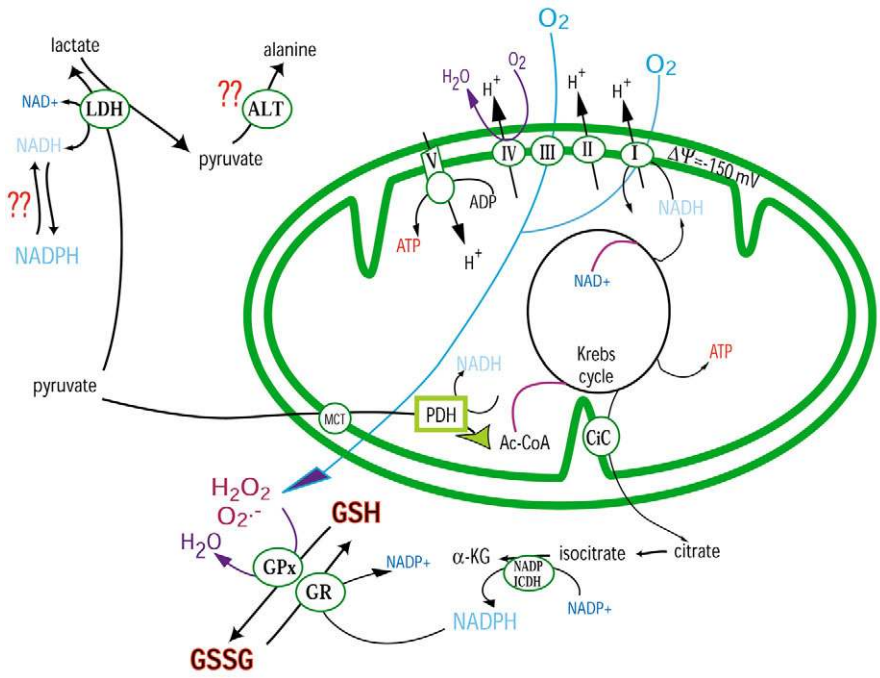

Fig. 7. Redox metabolism in the mouse zygote. Schematic representation of the metabolic pathways producing NADH, NADPH and GSH functioning in the cytosol and mitochondria of a mouse oocyte. See discussion for details. GSH, reduced glutathione, GSSG, oxidised glutathione, GPx, glutathione peroxidase, GR, glutathione reductase; H_2O_2, hydrogen peroxide; $O_2^{\cdot -}$, superoxide.

quite distinct from that of mature somatic cells (Jain et al., 2003; Tian et al., 1999; Tian et al., 1998) or *Xenopus* oocytes (Nutt et al., 2005), in which the PPP is a major provider of NADPH. Stimulation of the PPP after sperm entry has been described in the mouse (Urner and Sakkas, 2005); thus, PPP might have a more significant role in the regulation of NADPH levels in fertilised oocytes, a hypothesis we are now investigating.

Intracellular metabolism of lactate in mouse oocytes

We have found that lactate increases global NAD(P)H autofluorescence without affecting mitochondrial autofluorescence, suggesting that it is metabolised in the cytosol but not by the mitochondria. That the powerful effect of added lactate in reducing the cytosolic redox state was blocked by oxamate, an LDH inhibitor, confirms the key role of LDH in the supply of NADH and pyruvate in the mouse oocyte (Lane and Gardner, 2000) (Fig. 7). Oxamate alone also promoted oxidation of cytosolic NAD(P)H in oocytes incubated in complete KSOM/AA, further demonstrating a major role for LDH in supplying cytosolic NADH in the resting oocyte.

Surprisingly, lactate-derived pyruvate seems to be minimally metabolised by the mitochondria, as mitochondrial autofluorescence was never affected by lactate addition, even after a delay. This suggests the presence of discrete pools of pyruvate inside the oocyte: one from the bathing medium, which is rapidly metabolised by the mitochondria (see below), while a second pool derived from lactate is poorly used by the mitochondria. Such intracellular compartmentation of pyruvate pools has been described in neuronal and glial cells (Cruz et al., 2001; Zwingmann et al., 2001). Strikingly, in astrocytes, pyruvate derived from cytosolic alanine is poorly transported into mitochondria but is preferentially converted to lactate, which is exported from the cell (Zwingmann et al., 2001). It seems plausible that lactate-derived pyruvate may be preferentially converted in the cytosol to alanine by alanine aminotransferase (ALT) (Fig. 7), because: (1) preferential incorporation of carbon from lactate into alanine has been measured in mouse embryos (Quinn and Wales, 1973); (2) bovine oocytes contain strong ALT activity (Cetica et al., 2003); and (3) bovine and porcine embryos produce large amounts of alanine (Gopichandran and Leese, 2003; Humpherson et al., 2005). However, further studies are required to confirm such a hypothesis.

Finally, it is known that lactate alone is not able to support development from fertilisation, but only from the two-cell stage (Biggers et al., 1967; Johnson et al., 2003; Summers and Biggers, 2003). Our data showing that lactate-derived pyruvate does not support mitochondrial oxidative phosphorylation in the oocyte could explain why lactate is unable to support development from fertilisation.

Regulation of the intracellular NAD(P)H by pyruvate metabolism

Our data clearly demonstrate that pyruvate promotes oxidation of cytosolic NAD(P)H and reduction of mitochondrial $NAD(P)^+$ and FAD^{++}. Thus, as in most cell types, pyruvate is, in the mouse oocyte, a cytosolic oxidant but a mitochondrial reductant. These effects of pyruvate on mitochondrial redox state are consistent with its central role in fuelling oxidative phosphorylation and ATP production in the mouse oocyte (Fig. 7) (Leese, 2002; Johnson et al., 2003; Dumollard et al., 2004).

Two metabolic pathways might explain the cytosolic oxidation by pyruvate; pyruvate can be metabolised by LDH and ME to consume NADH and NADPH, respectively (Fig. 1) (Stryer, 1970). Our observations suggest that the reduction of pyruvate to lactate by LDH is the major pathway present in oocytes, as the oxidant effects of pyruvate were independent of mitochondrial activity and were completely blocked by inhibition of LDH. Further, we found no evidence for cytosolic ME activity, as addition of a permeant malate analogue had no effect on NAD(P)H levels while causing a reduction of mitochondrial FAD^{++}.

Our data suggest that a delicate balance is maintained between cytosolic and mitochondrial metabolism of pyruvate, such that any disruption of that balance strongly impacts on the redox state. Indeed, when uptake of pyruvate into mitochondria was blocked, a sharp oxidation of cytosolic NADH was observed. This poise of

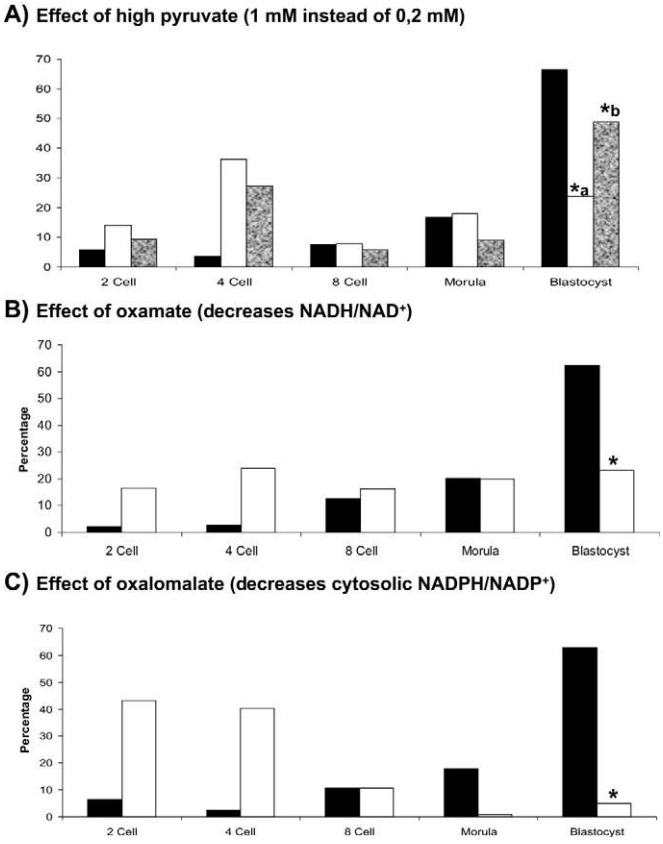

Fig. 8. Regulation of early development by the redox potential. (**A**) Effect of high pyruvate (1 mmol/l) on early development of mouse embryo. The bars indicate the percentage of embryos at each stage of development observed after 5 days of culture in control conditions (black bars), in H-KSOM/AA containing 1 mmol/l pyruvate (white bars) and in H-KSOM/AA containing 1 mmol/l pyruvate and 8 mmol/l TEMPO (stippled bars). Asterisk a (*a) indicates that this value is significantly different from the control value. Asterisk b (*b) indicates that this value is significantly different from the value of the white bar (high pyruvate treatment). (**B**) Effect of oxamate on early development of mouse embryos. Black bars: control condition. White bars: culture in the presence of 10 mmol/l oxamate. Asterisk indicates that this value is significantly different from the control value. (**C**) Effect of oxalomalate on early development of mouse embryos. Black bars: control condition. White bars: culture in the presence of 9 mmol/l oxalomalate. Asterisk indicates that this value is significantly different from the control value. P=0.05.

cytosolic pyruvate set by pyruvate in the medium and its transport into mitochondria is crucial for optimising energy balance and the cytosolic NADH:NAD^+ ratio.

Our data further suggest that mitochondrial metabolism of pyruvate also regulates the cytosolic NADPH:$NADP^+$ ratio. We observed that blocking NADP-ICDH in oocytes incubated in complete KSOM/AA decreased cytosolic NAD(P)H, suggesting that NADP-ICDH activity maintains cytosolic NADPH levels. As shown in Fig. 7, NADP-ICDH couples the reduction of $NADP^+$ to the conversion of isocitrate to α-ketoglutarate (α-KG) in the cytosol. Such isocitrate originates from citrate synthesised solely by the Krebs cycle before being exported from the mitochondria [a process called anaplerosis (MacDonald et al., 2005) (Fig. 7)]. Therefore the observation that NADP-ICDH activity maintains cytosolic NADPH levels suggests that mitochondrial pyruvate metabolism produces citrate in the oocyte. The earlier finding that mouse zygotes contain high levels of intracellular citrate supplied by the metabolism of exogenous pyruvate (Barbehenn et al., 1974) supports such a hypothesis. This pathway plays a primordial role in providing cytosolic NADPH in several somatic cell types (Mallet and Sun, 2003; Yang and Park, 2003; MacDonald et al., 2005). Given the lack of activity of the PPP in mouse oocytes, this pathway may represent a vital supply of cytosolic NADPH in the mouse oocyte and early embryo, but further experiments are needed to confirm such a hypothesis.

Together our observations show that both cytosolic and mitochondrial metabolism of pyruvate regulates cytosolic NADPH and NADH levels via cytosolic LDH and cytosolic NADP-ICDH. The diverse metabolism of pyruvate in the mouse oocyte has a dual impact on the intracellular oxidant load, as NADPH has an antioxidant action (see below) but mitochondrial NADH may promote mitochondrial ROS production (Fig. 7) (Balaban et al., 2005; Xu and Finkel, 2002).

GSH metabolism in mouse oocytes and embryos

A major role for intracellular NADPH is to fuel regeneration of GSH via the glutaredoxin-glutathione reductase (Grx-GR) system and the thioredoxin system (MacDonald et al., 2005; Holmgren et al., 2005). By measuring autofluorescence and GSH levels in the same oocyte, we were able to determine the relationships between NAD(P)H and GSH during the first stages of development. Our observations demonstrate that, in mouse oocytes, intracellular NADPH is consumed to regenerate GSH by the Grx-GR system, as direct oxidation of GSH by diamide provoked a concomitant oxidation of NAD(P)H, whereas GR inhibition that depleted GSH levels increased NAD(P)H.

Measuring NAD(P)H and GSH before maturation, before fertilisation and after the first cleavage revealed that GSH increases during maturation and then decreases during development, as described previously (for a review, see Luberda, 2005). However, NAD(P)H levels were constant during maturation and decreased after fertilisation. The finding that the increase in GSH observed during maturation is not accompanied by an increase in NAD(P)H levels suggests that the production of GSH during maturation depends modestly on NADPH availability. By contrast, the decrease in GSH observed after fertilisation was accompanied by a concomitant decrease in NAD(P)H levels, suggesting that GSH production is limited by NADPH availability. These two hypotheses are consistent with the earlier findings that GSH production relies crucially on ATP-dependent de novo synthesis during oocyte maturation, whereas de novo synthesis of GSH is switched off after fertilisation (Gardiner and Reed, 1995a; Luberda, 2005). By contrast, NADPH-dependent regeneration of GSH by the GR-Grx system operates during both maturation and early development (Gardiner and Reed, 1995b; Luberda, 2005). Thus, NADPH levels may be more crucial for the maintenance of GSH levels during early development than during oocyte maturation.

Together, our observations show that NADPH availability might set the GSH levels in the early embryo, thereby fuelling the antioxidant defence of the embryo, and suggest that early development is associated with an increase in oxidative stress that overpowers antioxidant defences, resulting in a decrease in both NADPH:$NADP^+$ and GSH:GSSG ratios.

Regulation of early development by the redox potential

The detrimental effect of oxidative stress and the protection exerted by GSH on early development are now well established (Johnson and Nasr-Esfahani, 1994; Gardner et al., 2002; Guerin et al., 2001;

Leese, 2002; Luberda, 2005). However, the impact on development of the redox potential – set in the mouse zygote mainly by pyruvate and lactate metabolism – is more difficult to infer due to its dual action on oxidative stress. The observation that high pyruvate (1 mmol/l) in the culture medium has a detrimental impact on development that can be reversed by an antioxidant shows that pyruvate metabolism causes damaging oxidative stress in the mouse embryo. The oxidant action of pyruvate on the embryo is illustrated by the fact that, despite the generation of NADPH from pyruvate via anaplerosis and NADP-ICDH, increasing pyruvate results in a net oxidation of cytosolic NAD(P)H and a net increase in mitochondrial NADH, which increases mitochondrial ROS production (Fig. 7). Therefore, even though pyruvate can detoxify ROS by directly scavenging hydrogen peroxide (Constantopoulos and Barranger, 1984), such antioxidant action of pyruvate is surpassed by the complex metabolism of pyruvate in the oocyte, which increases the intracellular oxidant load.

The main impact of cytosolic NADPH on oxidative stress is to maintain antioxidant defence, as it is mainly used to regenerate GSH in the mouse oocyte. It is important to note that mammalian oocytes do not appear to possess NAD(P)H oxidase activity as alternative generators of ROS and H_2O_2 (Geiszt and Leto, 2004). The role of NADH on oxidative stress in mouse oocytes is less straightforward, as NADH is a direct antioxidant (Kirsch and De Groot, 2001) but its oxidation by the respiratory chain generates ROS (Xu and Finkel, 2002; Balaban et al., 2005) (Fig. 7). Such an oxidant action of pyruvate-derived NADH in the mitochondria promotes cell senescence in human diploid fibroblasts (Xu and Finkel, 2002). Similarly, in the mouse oocyte, an oxidant action of pyruvate in the mitochondria may overwhelm the antioxidant defence of the embryo, thereby impairing development.

Maintenance of cytosolic NADH and NADPH levels by LDH and NADP-ICDH seems crucial for early development of the mouse, even when mitochondrial respiration is low (i.e. when pyruvate is low), as inhibiting each enzyme drastically impaired development. As depleting NADH also depletes NADPH (Fig. 5), it is not possible to differentiate between their respective roles. Further studies are necessary to determine whether these treatments impair early development by increasing the oxidant load experienced by the embryos.

In conclusion, our study describes for the first time how metabolism of exogenous substrates regulates the intracellular redox potential in the mouse oocyte and how such a tightly regulated redox potential supports efficient early development. This work explains the roles played by metabolites present in culture media and will inform future progress in the physiological characterisation of mammalian early development.

The authors would like to thank Guillaume Halet for his precious help during the course of the study. Work in the laboratories of John Carroll and Michael Duchen is supported by the MRC and the Wellcome Trust, respectively.

References

Akella, S. S. and Harris, C. (1999). Pyridine nucleotide flux and glutathione oxidation in the cultured rat conceptus. *Reprod. Toxicol.* **13**, 203-213.
Balaban, R. S., Nemoto, S. and Finkel, T. (2005). Mitochondria, oxidants, and aging. *Cell* **120**, 483-495.
Barbehenn, E. K., Wales, R. G. and Lowry, O. H. (1974). The explanation for the blockade of glycolysis in early mouse embryos. *Proc. Natl. Acad. Sci. USA* **71**, 1056-1060.
Biggers, J. D., Whittingham, D. G. and Donahue, R. P. (1967). The pattern of energy metabolism in the mouse oocyte and zygote. *Proc. Natl. Acad. Sci. USA* **58**, 560-567.
Biggers, J. D., McGinnis, L. K. and Raffin, M. (2000). Amino acids and preimplantation development of the mouse in protein-free potassium simplex optimized medium. *Biol. Reprod.* **63**, 281-293.
Cetica, P., Pintos, L., Dalvit, G. and Beconi, M. (2002). Activity of key enzymes involved in glucose and triglyceride catabolism during bovine oocyte maturation in vitro. *Reproduction* **124**, 675-681.
Cetica, P., Pintos, L., Dalvit, G. and Beconi, M. (2003). Involvement of enzymes of amino acid metabolism and tricarboxylic acid cycle in bovine oocyte maturation in vitro. *Reproduction* **126**, 753-763.
Comizzoli, P., Urner, F., Sakkas, D. and Renard, J. P. (2003). Up-regulation of glucose metabolism during male pronucleus formation determines the early onset of the s phase in bovine zygotes. *Biol. Reprod.* **68**, 1934-1940.
Constantopoulos, G. and Barranger, J. A. (1984). Nonenzymatic decarboxylation of pyruvate. *Anal. Biochem.* **139**, 353-358.
Correa, F., Garcia, N., Garcia, G. and Chavez, E. (2003). Dehydroepiandrosterone as an inducer of mitochondrial permeability transition. *J. Steroid Biochem. Mol. Biol.* **87**, 279-284.
Cruz, F., Villalba, M., Garcia-Espinosa, M. A., Ballesteros, P., Bogonez, E., Satrustegui, J. and Cerdan, S. (2001). Intracellular compartmentation of pyruvate in primary cultures of cortical neurons as detected by (13)C NMR spectroscopy with multiple (13)C labels. *J. Neurosci. Res.* **66**, 771-781.
Del Prete, E., Lutz, T. A. and Scharrer, E. (2004). Inhibition of glucose oxidation by alpha-cyano-4-hydroxycinnamic acid stimulates feeding in rats. *Physiol. Behav.* **80**, 489-498.
Dickinson, D. A. and Forman, H. J. (2002). Glutathione in defense and signaling: lessons from a small thiol. *Ann. N. Y. Acad. Sci.* **973**, 488-504.
Downs, S. M., Humpherson, P. G. and Leese, H. J. (1998). Meiotic induction in cumulus cell-enclosed mouse oocytes: involvement of the pentose phosphate pathway. *Biol. Reprod.* **58**, 1084-1094.
Duchen, M. R., Surin, A. and Jacobson, J. (2003). Imaging mitochondrial function in intact cells. *Methods Enzymol.* **361**, 353-389.
Dumollard, R., Hammar, K., Porterfield, M., Smith, P. J., Cibert, C., Rouviere, C. and Sardet, C. (2003). Mitochondrial respiration and Ca^{2+} waves are linked during fertilisation and meiosis completion. *Development* **130**, 683-692.
Dumollard, R., Marangos, P., Fitzharris, G., Swann, K., Duchen, M. and Carroll, J. (2004). Sperm-triggered [Ca2+] oscillations and Ca2+ homeostasis in the mouse egg have an absolute requirement for mitochondrial ATP production. *Development* **131**, 3057-3067.
Dumollard, R., Duchen, M. and Sardet, C. (2006a). Calcium signals and mitochondria at fertilisation. *Semin. Cell Dev. Biol.* **17**, 314-323.
Dumollard, R., Duchen, M. and Carroll, J. (2006b). The role of mitochondrial function in the oocyte and embryo. *Curr. Top. Dev. Biol.* (in press).
Fissore, R. A., Kurokawa, M., Knott, J., Zhang, M. and Smyth, J. (2002). Mechanisms underlying oocyte activation and postovulatory ageing. *Reproduction* **124**, 745-754.
Gardiner, C. S. and Reed, D. J. (1995a). Glutathione redox cycle-driven recovery of reduced glutathione after oxidation by tertiary-butyl hydroperoxide in preimplantation mouse embryos. *Arch. Biochem. Biophys.* **321**, 6-12.
Gardiner, C. S. and Reed, D. J. (1995b). Synthesis of glutathione in the preimplantation mouse embryo. *Arch. Biochem. Biophys.* **318**, 30-36.
Gardner, D. K., Lane, M. and Schoolcraft, W. B. (2002). Physiology and culture of the human blastocyst. *J. Reprod. Immunol.* **55**, 85-100.
Geiszt, M. and Leto, T. L. (2004). The Nox family of NAD(P)H oxidases: host defense and beyond. *J. Biol. Chem.* **279**, 51715-51718.
Ghezzi, P. (2005). Oxidoreduction of protein thiols in redox regulation. *Biochem. Soc. Trans.* **33**, 1378-1381.
Gopichandran, N., and Leese, H. J. (2003). Metabolic characterization of the bovine blastocyst, inner cell mass, trophectoderm and blastocoel fluid. *Reproduction* **126**, 299-308.
Guerin, P., El Mouatassim, S. and Menezo, Y. (2001). Oxidative stress and protection against reactive oxygen species in the pre-implantation embryo and its surroundings. *Hum. Reprod. Update* **7**, 175-189.
Hildebrand, J. D. and Soriano, P. (2002). Overlapping and unique roles for C-terminal binding protein 1 (CtBP1) and CtBP2 during mouse development. *Mol. Cell. Biol.* **22**, 5296-5307.
Holmgren, A., Johansson, C., Berndt, C., Lonn, M. E., Hudemann, C. and Lillig, C. H. (2005). Thiol redox control via thioredoxin and glutaredoxin systems. *Biochem. Soc. Trans.* **33**, 1375-1377.
Houghton, F. D., Thompson, J. G., Kennedy, C. J. and Leese, H. J. (1996). Oxygen consumption and energy metabolism of the early mouse embryo. *Mol. Reprod. Dev.* **44**, 476-485.
Humpherson, P. G., Leese, H. J. and Sturmey, R. G. (2005). Amino acid metabolism of the porcine blastocyst. *Theriogenology* **64**, 1852-1866.
Imai, S., Johnson, F. B., Marciniak, R. A., McVey, M., Park, P. U. and Guarente, L. (2000). Sir2: an NAD-dependent histone deacetylase that connects chromatin silencing, metabolism, and aging. *Cold Spring Harb. Symp. Quant. Biol.* **65**, 297-302.
Jain, M., Brenner, D. A., Cui, L., Lim, C. C., Wang, B., Pimentel, D. R., Koh, S., Sawyer, D. B., Leopold, J. A., Handy de Loscalzo, J. et al. (2003). Glucose-6-phosphate dehydrogenase modulates cytosolic redox status and contractile phenotype in adult cardiomyocytes. *Circ. Res.* **93**, e9-e16.
Johnson, M. H. and Nasr-Esfahani, M. H. (1994). Radical solutions and cultural problems: could free oxygen radicals be responsible for the impaired

development of preimplantation mammalian embryos in vitro? *BioEssays* **16**, 31-38.
Johnson, M. T., Mahmood, S. and Patel, M. S. (2003). Intermediary metabolism and energetics during murine early embryogenesis. *J. Biol. Chem.* **278**, 31457-31460.
Keelan, J., Allen, N. J., Antcliffe, D., Pal, S. and Duchen, M. R. (2001). Quantitative imaging of glutathione in hippocampal neurons and glia in culture using monochlorobimane. *J. Neurosci. Res.* **66**, 873-884.
Kirsch, M. and De Groot, H. (2001). NAD(P)H, a directly operating antioxidant? *FASEB J.* **15**, 1569-1574.
Kosower, N. S. and Kosower, E. M. (1995). Diamide: an oxidant probe for thiols. *Meth. Enzymol.* **251**, 123-133.
Lane, M. and Gardner, D. K. (2000). Lactate regulates pyruvate uptake and metabolism in the preimplantation embryo. *Biol. Reprod.* **62**, 16-22.
Lane, M. and Gardner, D. K. (2005). Mitochondrial malate-aspartate shuttle regulates mouse embryo nutrient consumption. *J. Biol. Chem*. **280**, 18361-18367.
Leese, H. J. (1995). Metabolic control during preimplantation mammalian development. *Hum. Reprod. Update* **1**, 63-72.
Leese, H. J. (2002). Quiet please, do not disturb: a hypothesis of embryo metabolism and viability. *BioEssays* **24**, 845-849.
Liu, H., Colavitti, R., Rovira, I. I. and Finkel, T. (2005). Redox-dependent transcriptional regulation. *Circ. Res.* **97**, 967-974.
Liu, L. and Keefe, D. L. (2000). Cytoplasm mediates both development and oxidation-induced apoptotic cell death in mouse zygotes. *Biol. Reprod.* **62**, 1828-1834.
Liu, L., Trimarchi, J. R. and Keefe, D. L. (2000). Involvement of mitochondria in oxidative stress-induced cell death in mouse zygotes. *Biol. Reprod.* **62**, 1745-1753.
Luberda, Z. (2005). The role of glutathione in mammalian gametes. *Reprod. Biol.* **5**, 5-17.
MacDonald, M. J., Fahien, L. A., Brown, L. J., Hasan, N. M., Buss, J. D. and Kendrick, M. A. (2005). Perspective: emerging evidence for signaling roles of mitochondrial anaplerotic products in insulin secretion. *Am. J. Physiol. Endocrinol. Metab.* **288**, E1-E15.
Mallet, R. T. and Sun, J. (2003). Antioxidant properties of myocardial fuels. *Mol. Cell. Biochem.* **253**, 103-111.
McBurney, M. W., Yang, X., Jardine, K., Hixon, M., Boekelheide, K., Webb, J. R., Lansdorp, P. M. and Lemieux, M. (2003). The mammalian SIR2alpha protein has a role in embryogenesis and gametogenesis. *Mol. Cell. Biol.* **23**, 38-54.
Nutt, L. K., Margolis, S. S., Jensen, M., Herman, C. E., Dunphy, W. G., Rathmell, J. C. and Kornbluth, S. (2005). Metabolic regulation of oocyte cell death through the CaMKII-mediated phosphorylation of caspase-2. *Cell* **123**, 89-103.
Quinn, P. and Wales, R. G. (1973). Uptake and metabolism of pyruvate and lactate during preimplantation development of the mouse embryo in vitro. *J. Reprod. Fertil.* **35**, 273-287.
Stryer, L. (1970). *Biochemistry* (2nd edn). Freeman and Company.
Summers, M. C. and Biggers, J. D. (2003). Chemically defined media and the culture of mammalian preimplantation embryos: historical perspective and current issues. *Hum. Reprod. Update* **9**, 557-582.
Tarin, J. J. (1996). Potential effects of age-associated oxidative stress on mammalian oocytes/embryos. *Mol. Hum. Reprod.* **2**, 717-724.
Tian, W. N., Braunstein, L. D., Pang, J., Stuhlmeier, K. M., Xi, Q. C., Tian, X. and Stanton, R. C. (1998). Importance of glucose-6-phosphate dehydrogenase activity for cell growth. *J. Biol. Chem.* **273**, 10609-10617.
Tian, W. N., Braunstein, L. D., Apse, K., Pang, J., Rose, M., Tian, X. and Stanton, R. C. (1999). Importance of glucose-6-phosphate dehydrogenase activity in cell death. *Am. J. Physiol.* **276**, C1121-C1131.
Urner, F. and Sakkas, D. (2005). Involvement of the pentose phosphate pathway and redox regulation in fertilization in the mouse. *Mol. Reprod. Dev.* **70**, 494-503.
Wales, R. G. and Whittingham D. G. (1971). Decompositiopn of sodium pyruvate in culture media stored at 5C and its effects on the development of the preimplantation mouse embryo. *J. Reprod. Fertil.* **24**, 126.
Wilkinson, J. H. and Walter, S. J. (1972). Oxamate as a differential inhibitor of lactate dehydrogenase isoenzymes. *Enzyme* **13**, 170-176.
Xu, D. and Finkel, T. (2002). A role for mitochondria as potential regulators of cellular life span. *Biochem. Biophys. Res. Commun.* **294**, 245-248.
Yang, H. W., Hwang, K. J., Kwon, H. C., Kim, H. S., Choi, K. W. and Oh, K. S. (1998). Detection of reactive oxygen species (ROS) and apoptosis in human fragmented embryos. *Hum. Reprod.* **13**, 998-1002.
Yang, J. H. and Park, J. W. (2003). Oxalomalate, a competitive inhibitor of NADP+-dependent isocitrate dehydrogenase, enhances lipid peroxidation-mediated oxidative damage in U937 cells. *Arch. Biochem. Biophys.* **416**, 31-37.
Zhang, Q., Piston, D. W. and Goodman, R. H. (2002). Regulation of corepressor function by nuclear NADH. *Science* **295**, 1895-1897.
Zwingmann, C., Richter-Landsberg, C. and Leibfritz, D. (2001). 13C isotopomer analysis of glucose and alanine metabolism reveals cytosolic pyruvate compartmentation as part of energy metabolism in astrocytes. *Glia* **34**, 200-212.